[O II] Emission, Eigenvector 1, and Orientation in Radio-quiet Quasars

Permanent link

http://nrs.harvard.edu/urn-3:HUL.InstRepos:30248640

Share Your Story

The Harvard community has made this article openly available.
Please share how this access benefits you. Submit a story.

Accessibility

[O II] EMISSION, EIGENVECTOR 1, AND ORIENTATION IN RADIO-QUIET QUASARS

J. KURASZKIEWICZ,[1] AND B. J. WILKES
Harvard-Smithsonian Center for Astrophysics, Cambridge, MA 02138

W. N. BRANDT
Department of Astronomy and Astrophysics, Pennsylvania State University, University Park, PA 16802

AND

M. VESTERGAARD[2]
Ohio State University, Columbus, OH 43120

ABSTRACT

We present supportive evidence that the Boroson & Green eigenvector 1 is not driven by source orientation and further that both [O III] $\lambda5007$ and [O II] $\lambda3727$ are isotropically emitted in the radio-quiet sample of bright quasar survey (BQS) quasars, contrary to results found for radio-loud active galactic nuclei (AGNs). Studies of optical emission lines in quasars have revealed a striking set of correlations between various emission-line properties, known as the Boroson & Green eigenvector 1. Until recently it was generally accepted that eigenvector 1 does not depend on orientation, as it strongly correlates with [O III] $\lambda5007$ emission, thought to be an isotropic property. However, recent studies of radio-loud AGNs have questioned the isotropy of [O III] emission and concluded that [O II] $\lambda3727$ emission is isotropic. In this paper we investigate the relation between eigenvector 1 and [O II] emission in radio-quiet BQS quasars and readdress the issue of orientation as the driver of eigenvector 1. We account for the small blue bump present at [O II] wavelengths and subtract Fe II emission that contaminates [O III] emission. We find significant correlations between eigenvector 1 and orientation-independent [O II] emission, which implies that orientation does not drive eigenvector 1. The luminosities and equivalent widths of [O III] and [O II] correlate with one another, and the range in luminosities and equivalent widths is similar. This suggests that our radio-quiet BQS quasar sample is largely free of orientation-dependent obscuration and/or ionization effects. We conclude that neither the [O III] emission nor the [O II]/[O III] ratio are dependent on orientation in radio-quiet quasars, contrary to recent results found for radio-loud quasars.

Subject headings: galaxies: active — quasars: emission lines

1. INTRODUCTION

Studies of optical emission lines in quasars have revealed some striking correlations that may well be related to the fundamental properties of the accreting black hole system. Boroson & Green (1992, hereafter BG92) performed a principal component analysis (PCA) on the bright quasar survey (BQS) quasar sample (Schmidt & Green 1983) and showed that the primary eigenvector (hereafter EV1), which was responsible for ~30% of the variance in the data, was anticorrelated with various measures of Fe II $\lambda4570$ strength (equivalent width and Fe II/Hβ ratio), correlated with [O III] $\lambda5007$ strength (luminosity and peak) and Hβ FWHM, and anticorrelated with the blue asymmetry of the Hβ line. It was later found that these optical line properties correlate with UV properties (C III] width, Si III]/C III] ratio, C IV and N V strength; Wills et al. 1999, Kuraszkiewicz et al. 2000) and with soft X-ray properties (luminosity and spectral index; BG92, Corbin 1993, Laor et al. 1994, 1997). Recently, Brandt & Boller (1998) showed that the correlations between EV1 and the X-ray properties are stronger than those with the individual line parameters, suggesting that EV1 has a more fundamental physical meaning. A number of physical parameters have been suggested to drive EV1, including accretion rate, orientation, and black hole spin.

BG92 and Boroson (1992) argued that EV1 is not driven by an orientation effect (i.e., some anisotropic property), despite the strong dependence on Hβ line width, as it is strongly correlated with the [O III] $\lambda5007$ (hereafter [O III]) luminosity, which was assumed to be isotropic. However, the isotropy of the [O III] emission in other AGNs has since been called into question. Jackson & Browne (1990) studied a sample of powerful narrow-line radio galaxies and radio-loud quasars, which, in the context of unified models (e.g., Antonucci 1993), are considered to be the same type of object viewed from different angles to the radio axis. The [O III] line luminosity of the narrow-line radio galaxies (viewed edge-on) is lower by 5–10 times than that of the quasars, matched in redshift and extended radio luminosity. This result was surprising. It was expected that the [O III] emission would be the same in both samples, as it was thought to originate from distances large enough to be unaffected by obscuring material from the dusty torus. Hes, Barthel, & Fosbury (1996) found that radio-loud quasars and powerful narrow-line radio galaxies show no difference in [O II] $\lambda3727$ (hereafter [O II]) emission, suggesting that [O II] emission, and not [O III] emission, is isotropic. As [O III] has a higher critical density and higher ionization potential and hence lies nearer to the central engine, this difference can be explained if the [O III] emission region extends to sufficiently small radii to be obscured by the dusty torus when the active nucleus is viewed "edge-on." Support for this scenario was provided by the detection of [O III] emission in polarized light in four out of seven radio galaxies (one also showing [O II] polarization), while a

---

sample of radio-loud quasars showed none (di Serego Alighieri et al. 1997). Polarized [O III] emission has also been observed in NGC 4258 (Wilkes et al. 1995; Barth et al. 1999), a Seyfert galaxy with an edge-on molecular disk surrounding the nucleus. Baker (1997, hereafter B97), studying a complete sample of low-frequency radio-selected quasars from the Molonglo quasar sample, found that the [O II]/[O III] ratio is anticorrelated with the radio core-to-lobe flux density ratio R, which is generally used as an orientation indicator. This again implies that [O III] is affected by dust absorption as the orientation becomes more edge-on. Similarly, the [O III] luminosity versus radio luminosity correlation shows a larger scatter than the similar [O II] versus radio correlation (Tadhunter et al. 1998) in the 2 Jy extended radio-selected sample (Wall & Peacock 1985a, 1985b). This additional scatter could again be explained by dust obscuration of the [O III] emission, although the authors prefer an interpretation in terms of the higher sensitivity of [O III] to the ionization parameter (Tadhunter et al. 1998).

If the central regions of radio-loud quasars and powerful radio galaxies are basically similar to the central regions of radio-quiet quasars (with the exception of the existence of the radio jets), then by analogy we would expect the behavior of the [O II] and [O III] lines to be similar in both classes. Indeed, Seyfert 1 galaxies, which in the unified model scenario correspond to the face-on Seyfert 2 galaxies, have higher [O III] luminosities than Seyfert 2 galaxies with comparable radio luminosity (Lawrence 1987; but see Keel et al. 1994, who find no difference in a sample of *IRAS*-selected Seyfert galaxies). This suggests that $L([O\ III])/L([O\ II])$ could be an orientation indicator not only in radio-loud but also in radio-quiet quasars. Similarly, Fe II emission strength and the broad line widths are strongly dependent on orientation in radio-loud quasi-stellar objects (QSOs) (e.g., Miley & Miller 1979; Wills & Browne 1986; Vestergaard, Wilkes, & Barthel 2000) with stronger Fe II and narrower lines in face-on sources. Again, by analogy, this suggests that the extreme EV1 objects, narrow-line Seyfert 1 galaxies, which have stronger Fe II emission and narrow lines, could also be face-on.

Given the strong evidence for anisotropic [O III] emission in radio-loud quasars, we present an investigation of the behavior of [O II] emission in a radio-quiet subset of the optically selected Palomar BQS sample to study the [O II] relation to EV1 in comparison with that of [O III]. This allows us to revisit the question of orientation as a driver of EV1, which will lead to a better understanding of the underlying physics driving the strongest set of emission-line correlations found to date for quasars, and so provide information on their central regions. We also compare the [O II] and [O III] emission in our radio-quiet, optically selected sample with radio-loud samples to investigate whether the behavior of [O II] and [O III] emission is similar in the two classes. Finally, we address the question of whether the [O II]/[O III] ratio is an orientation indicator in radio-quiet quasars.

2. OBSERVATIONS AND DATA REDUCTION

In order to carry out this investigation, the sample needs to cover a wide range of EV1 values. Since the [O III] luminosity ($M_{[O\ III]}$) is directly measurable and strongly correlates with EV1, our objects were selected to have either high or low [O III] luminosity, i.e., $M_{[O\ III]} < -28$ or

$M_{[O\ III]} > -25.5$ in the BG92 sample (see Fig. 1; however, a few radio-quiet quasars satisfying these selection criteria were not included in our sample because of a lack of observing time). Our sample consists of 11 objects with low [O III] luminosity and nine objects with high [O III] luminosity. We have obtained high signal-to-noise spectra of these quasars that include both the [O III] $\lambda5007$ and [O II] $\lambda3727$ lines. The observations were made between 1997 June and December with the FAST spectrograph on the 1.5 m Tillinghast telescope on Mount Hopkins in Arizona. A 300 groove mm^{-1} grating set to cover the wavelength range 3500–7500 Å was used with a 2″ aperture, yielding a resolution of ∼6 Å. Spectrophotometry was carried out, in photometric conditions, by observing each quasar twice, first through a large 5″ aperture and second through a small 2″ aperture with a longer exposure time to obtain high spectral resolution and signal-to-noise ratio. A standard star was observed through the wide aperture, at similar air mass, immediately before or after the quasar observation, to provide flux calibration. The data were reduced in the standard manner using IRAF[3] (see Tokarz & Roll 1997 for details). The continuum of the small-aperture data was then normalized to match the shape and absolute flux level of the large-aperture observation, yielding a final spectrum with a (judged from our experience) photometric accuracy of ∼5%. The observational details are given in Table 1, and the calibrated spectra are presented in Figure 2.

2.1. Fe II Subtraction

It has been shown (e.g., BG92) that Fe II emission is present in the form of broad humps of blended lines at 4450–4700 Å and 5150–5350 Å. This emission severely com-

---

[3] IRAF (Image Reduction and Analysis Facility) is distributed by the National Optical Astronomy Observatories, which are operated by AURA, Inc., under cooperative agreement with the National Science Foundation.
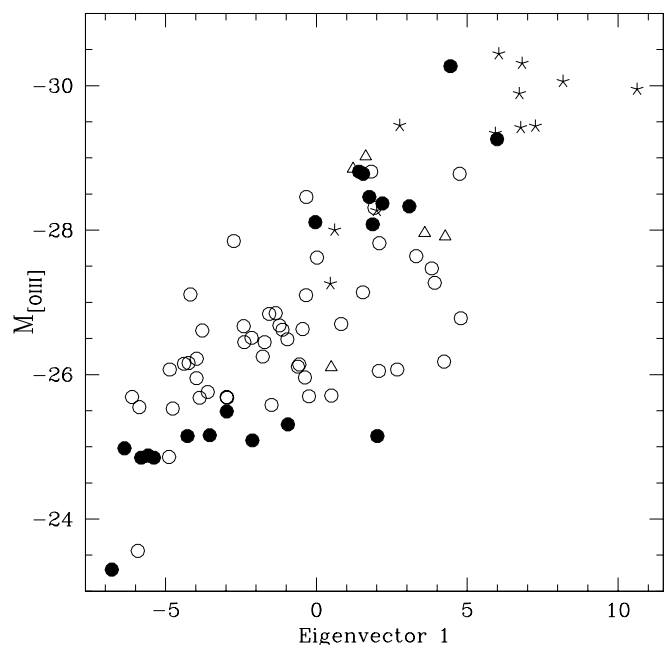

FIG. 1.—[O III] absolute magnitude ($M_{[O\ III]}$) from BG92 vs. BG92 EV1. Filled circles indicate the radio-quiet quasars in the current sample; open circles indicate radio-quiet QSOs in BG92; asterisks indicate steep spectrum radio-loud QSOs; and open triangles indicate flat spectrum radio-loud QSOs.

TABLE 1
Observational Details

Name	Other Name	R.A. (2000)	Decl. (2000)	z	UT Date (mm/dd/yy)	Exposure Time (s)
PG 0003+199......	Mrk 335	00 06 19.60	20 12 10.6	0.025	06/07/97	180
					06/07/97	660
PG 0026+129......		00 29 13.81	13 16 04.5	0.145	06/10/97	240
					06/10/97	900
PG 0052+251......		00 54 52.24	25 25 39.0	0.154	06/10/97	300
					06/10/97	1200
PG 0157+001......	Mrk 1014	01 59 50.28	00 23 40.8	0.163	06/10/97	300
					06/10/97	900
PG 0923+129......	Mrk 705	09 26 03.35	12 44 03.5	0.029	29/11/97	1200
					29/11/97	240
PG 0953+414......		09 56 52.46	41 15 22.0	0.234	29/11/97	300
					29/11/97	1020
PG 1049−005......		10 51 51.56	−00 51 16.8	0.360	31/12/97	360
					31/12/97	900
					31/12/97	900
PG 1116+215......	Ton 1388	11 19 08.77	21 19 17.9	0.177	05/06/97	240
					05/06/97	900
PG 1351+236......	Mrk 662	13 54 06.51	23 25 49.0	0.055	05/06/97	300
					05/06/97	900
					05/06/97	900
PG 1354+213......		13 56 32.94	21 03 51.1	0.301	05/06/97	300
					05/06/97	900
					05/06/97	900
PG 1402+261......	Ton 182	14 05 16.20	25 55 33.0	0.164	10/06/97	300
					10/06/97	900
					10/06/97	900
PG 1404+226......		14 06 21.98	22 23 46.7	0.098	10/06/97	300
					10/06/97	900
					10/06/97	900
PG 1415+451......		14 17 00.70	44 56 06.4	0.114	05/06/97	300
					05/06/97	900
					05/06/97	900
PG 1427+480......		14 29 43.14	47 47 26.9	0.221	11/06/97	420
					11/06/97	1200
					11/06/97	1200
PG 1519+226......		15 21 14.29	22 27 43.2	0.136	11/06/97	420
					11/06/97	1200
					11/06/97	1200
PG 1535+547......	I Zw 120	15 36 38.36	54 33 33.2	0.039	10/06/97	300
					10/06/97	660
					10/06/97	660
PG 1543+489......		15 45 30.31	48 46 09.0	0.400	10/06/97	360
					10/06/97	1080
					10/06/97	1080
PG 1552+085......		15 54 44.62	08 22 20.5	0.119	11/06/97	420
					11/06/97	1200
					11/06/97	1200
PG 1612+261......	Ton 256	16 14 13.29	26 04 16.4	0.131	10/06/97	360
					10/06/97	1020
					10/06/97	1020
PG 2304+042......	PB 5250	23 07 02.70	04 32 55.0	0.043	06/07/97	300
					06/07/97	840
					06/07/97	840

NOTE.—Units of right ascension are hours, minutes, and seconds, and units of declination are degrees, arcminutes, and arcseconds.

plicates measurements of emission-line strengths and widths. Around the [O III] $\lambda\lambda$4949, 5007 lines, a strong Fe II optical multiplet (42) consisting of three lines at 4924, 5018, and 5169 Å contaminates the [O III] emission. This contamination is particularly strong in the weak [O III] sources since, following EV1, these objects usually have strong Fe II emission (see BG92). At the [O II] λ3727 wavelength, a "small bump" (spanning 2000–4000 Å, which is a blend of Fe II lines with the Balmer continuum emission) resides, which has to be taken into account when making measurements of the [O II] line.

In our spectra we have fitted the underlying continuum with a power law using only those regions of the spectrum uncontaminated by the Fe II emission (4150–4270 Å and
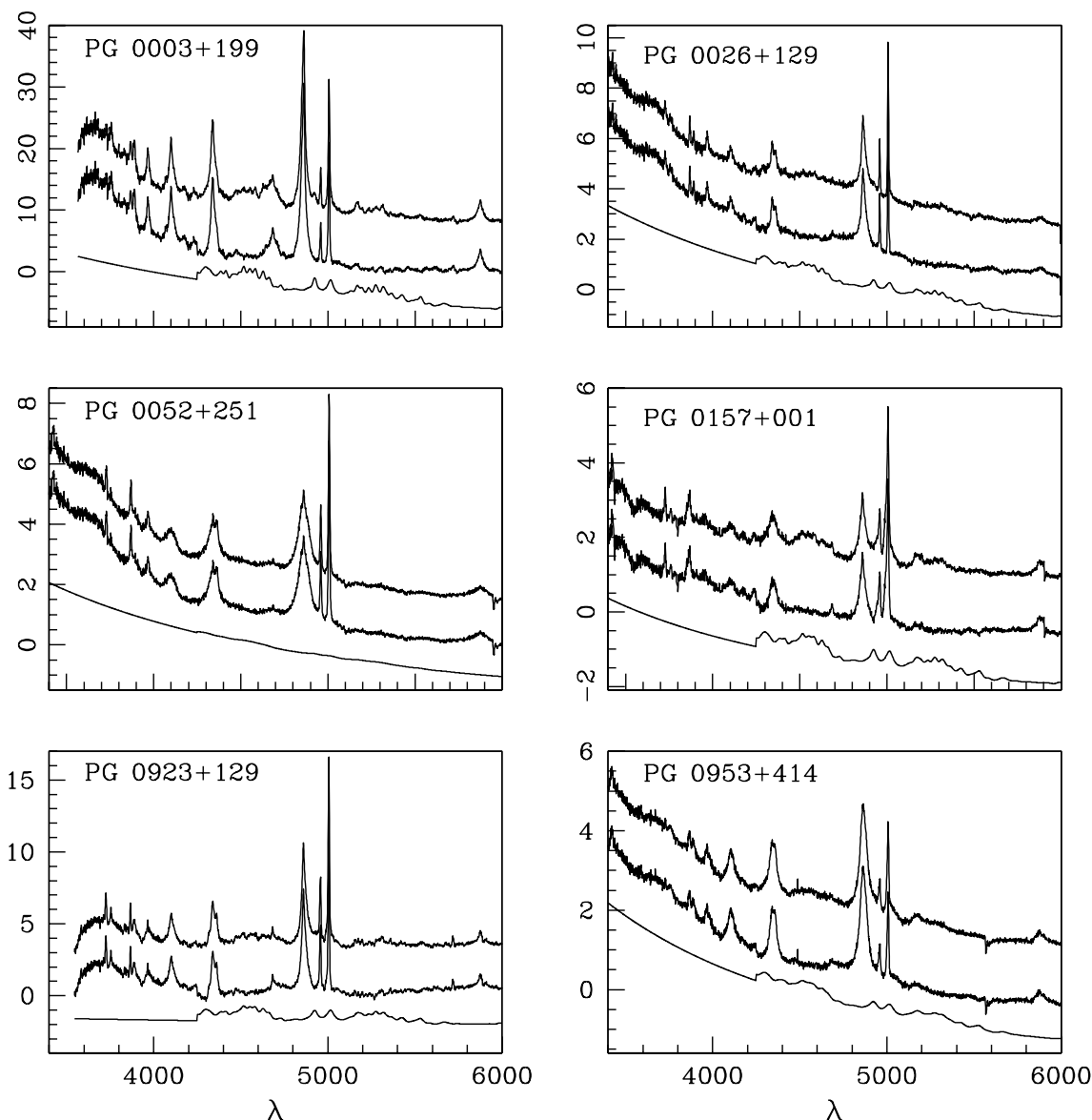
FIG. 2.—Observed and Fe II–subtracted spectra in the rest frame, in order of increasing right ascension. Only the wavelength range around the [O II] and [O III] lines is presented on a scale F_λ (in units of 10^{-15} ergs s^{-1} cm^{-2} Å^{-1}) as a function of λ(Å). The top spectrum is the observed spectrum, the middle is the Fe II–subtracted spectrum, and the bottom is the fitted Fe II model. The Fe II–subtracted spectrum and the Fe II model have been shifted downward by an arbitrary value for clarity.

6160–6280 Å). The underlying power-law continuum was then subtracted from each spectrum, and the Fe II emission was modeled using an optical (4247–7000 Å) Fe II template, kindly provided by Boroson (BG92). The template Fe II spectrum was broadened by convolving with Gaussian functions to multiple widths starting at 1000 km s^{-1} and separated by steps of 250 km s^{-1}. A two-dimensional iron emission model was constructed with line width as one dimension and rest wavelength as the other (see Vestergaard & Wilkes 2000). The iron emission in the object's spectrum was fitted by scaling this two-dimensional iron model to the iron emission on either side of the Hβ and [O III] lines. As a check-up and confirmation of this primary normalization, five additional scalings from 0.6 to 1.4 in steps of 0.2 were applied to each normalized iron model, and these were also compared to the object's spectrum. These additionally scaled models were never needed, confirming that the primary normalization was satisfactory and

adequate in each case. χ^2 statistics and residual flux measurements were used to determine the best-fit iron model, but manual inspection of how each model fits the spectrum and of the residual spectra was also necessary and was of high importance because of the complexity of QSO spectra. Once the best-fitting Fe II model was identified it was subtracted from the original QSO spectrum, allowing for an improved underlying continuum to be determined. The iteration over the Fe II model and continuum setting (Vestergaard & Wilkes 2000) was continued until little change was seen from one step to the next. Usually no more than two iterations were needed.

The best-fitting Fe II emission model was then subtracted from the QSO spectrum. The previously subtracted power-law continuum was then added back into the spectrum, giving an Fe II–subtracted spectrum. We present these spectra in Figure 2 along with the fitted Fe II models to each spectrum and the original, uncorrected QSO spectra.
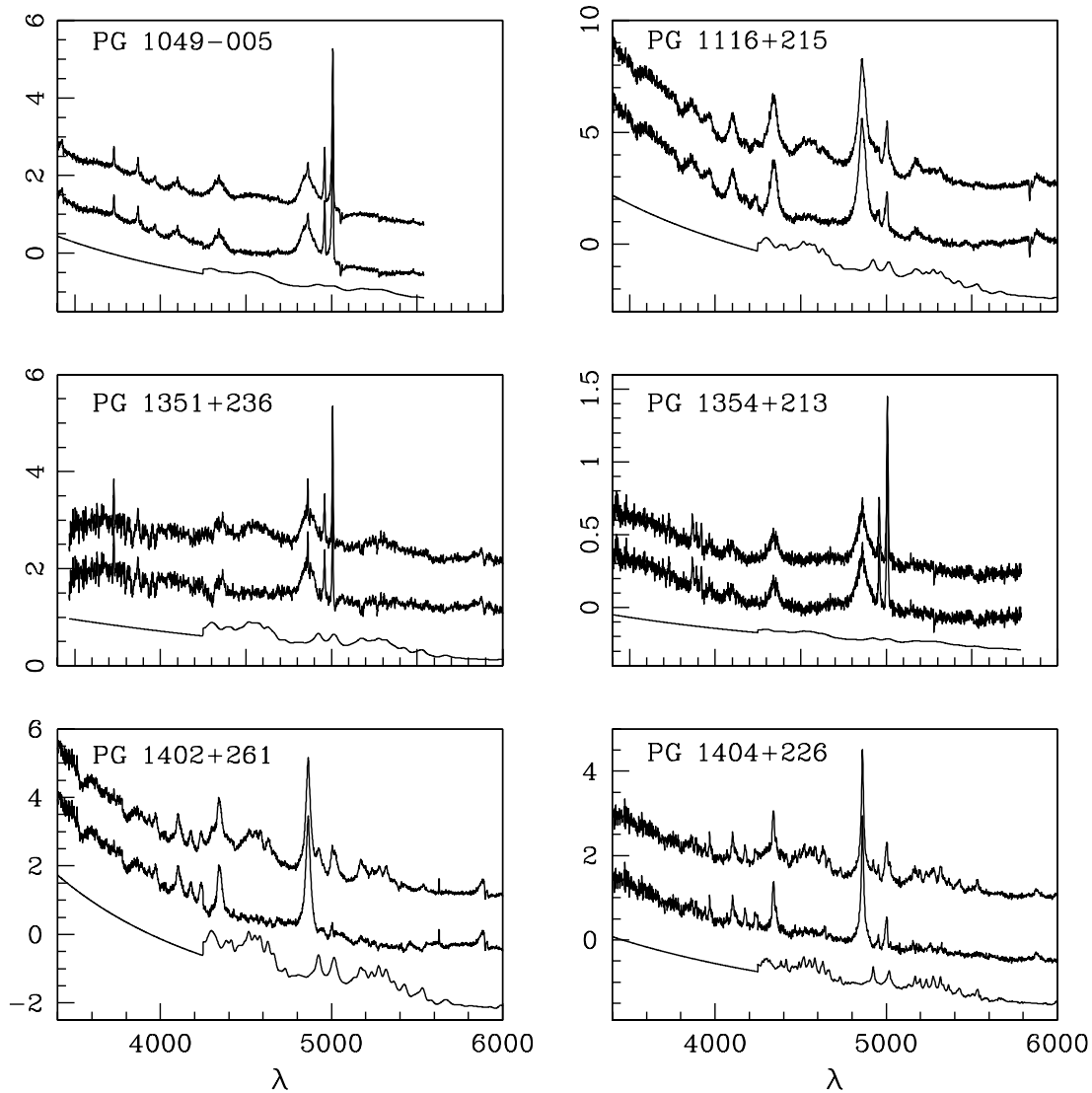
Fig. 2.—*Continued*

2.2. *Line Measurements*

The fluxes and equivalent widths (EWs) of the [O III] λ5007, [O II] λ3727, Hβ λ4861, and Fe II λ4570 lines (for comparison with the BG92 data) in the Fe II–subtracted spectra were measured using the SPLOT task in IRAF. For [O III] and Hβ we took the previously fitted, underlying power-law continuum and integrated the spectrum above this continuum and across the observed emission line (we used keystroke "e" in the IRAF SPLOT task). The flux and equivalent width of the Fe II λ4570 optical multiplet were measured in the 4434–4684 Å range across the fitted Fe II emission models. The equivalent widths and line luminosities of the emission lines are presented in Table 2. Our measurements of equivalent widths of Hβ, [O III], Fe II lines, and Fe II/Hβ agree with BG92 to within 30%, except where noted in the table.

The flux of the [O II] λ3727 line was measured by integrating the spectrum above a "local" continuum, i.e., the "small bump" (Fig. 3, *dashed line*; we did not subtract the "small bump," as it is not included in the template). The equivalent width was then defined as the ratio of the flux of the [O II] line estimated above the "small bump" to the

flux over the same wavelength range in the power-law continuum (Fig. 3, *solid line*; this took care of the contamination from the "small bump"). If, instead, the [O II] flux was divided by the local underlying continuum, as is more usual, then the equivalent width would be underestimated (by factors of up to ~5). A comparison of the equivalent widths obtained by the two methods (Fig. 4) illustrates a significant systematic shift in equivalent widths whose magnitude varies from source to source, emphasizing the need to take into account the small bump when measuring the [O II] line.

Our sample consists of luminous quasars ($M_B < -23$), which are generally not highly variable at optical wavelengths (e.g., Giveon et al. 1999). However, if any of the quasars had undergone a change of continuum from the time of BG92 observations, it would be seen in the differing EW([O III]) measurements (as the [O III] emitting region lies far enough from the central engine to be unaffected by the changing continuum on timescales of a few years). This may be the case for the following objects: PG 0026+129; PG 1427+480, where our EW([O III]) measurements are lower than those of BG92; and PG 1354+213, where our
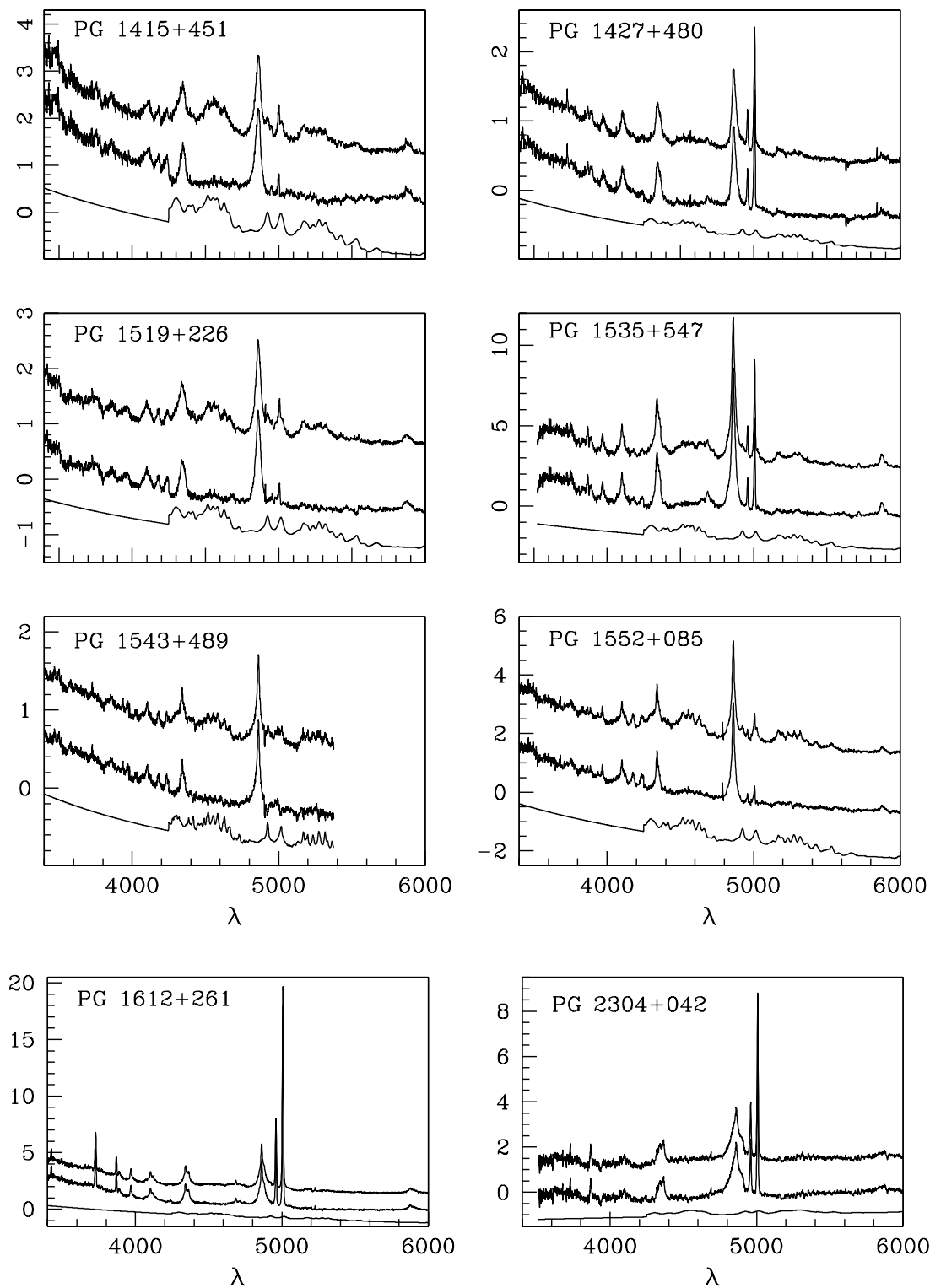
Fig. 2.—Continued

EW([O III]) is higher (see Table 2). These objects also show lower (or higher, respectively) EW(Hβ) and slightly lower (higher) EW(Fe II) measurements (although the change is less than 30% and hence not noted by an asterisk in Table 2). The Fe II/Hβ ratio did not differ significantly from BG92 in these objects. For PG 1543+489, BG92 quote EW([O III]) = 0, while we were able to measure this line in our spectra and obtained a value of 4.8 Å. A comparison of our line equivalent width measurements in PG 1612+261

and PG 2304+042 indicates that we have set the underlying continuum higher for PG 1612+261 and lower for PG 2304+042 and with a flatter slope, probably as a result of the wider wavelength range covered by our spectra, allowing a better continuum determination.

The line equivalent width measurements are influenced by the choice of aperture. BG92 used a 1.″5 aperture, while we use spectra obtained with a 2″ aperture and flux-calibrated using quasar spectra through a 5″ aperture

TABLE 2

LINE MEASUREMENTS[a,b]

PG QSO	EW([O III])	EW([O II])	EW(Hβ)	EW(Fe II)	Fe II/Hβ	L([O III])	L([O II])	[O II]/[O III]	EV1[c]
0003+199......	22.4	1.0	102.0	49.1	0.54	41.73	40.58	−1.15	−2.972
0026+129......	*13.6	5.0	*42.9	24.6	0.65	42.56	41.76	−0.80	2.189
0052+251......	33.5	5.0	91.7	*7.4	*0.09	42.80	41.78	−1.02	3.080
0157+001......	56.0	2.9	61.6	71.5	*1.36	42.82	41.86	−0.96	1.547
0923+129......	38.2	9.4	74.2	36.2	0.49	41.65	40.76	−0.89	−0.945
0953+414......	19.6	0.3	*90.9	33.3	*0.43	42.79	41.22	−1.57	1.414
1049−005......	45.0	4.0	75.9	39.2	0.60	43.28	42.34	−0.94	4.445
1116+215......	13.5	0.3	*91.9	*47.0	0.59	42.67	41.26	−1.41	−0.036
1351+236......	8.4	1.9	24.4	30.2	1.28	41.39	40.83	−0.56	−2.122
1354+213......	*51.6	6.1	*107.6	25.8	0.26	42.61	41.43	−1.18	1.867
1402+261......	3.2	0.3	85.7	101.4	1.44	41.67	41.00	−0.67	−5.389
1404+226......	9.9	<0.3	58.7	43.3	0.83	41.70	<40.39	−1.31	−6.362
1415+451......	2.9	<0.8	56.6	81.0	1.60	41.31	<40.96	−0.35	−6.784
1427+480......	*36.8	4.8	*95.0	43.1	0.51	42.51	41.52	−0.99	1.756
1519+226......	7.9	1.5	94.7	91.4	1.08	41.61	41.10	−0.51	−4.273
1535+547......	20.3	1.2	111.1	48.5	0.46	41.54	40.43	−1.11	−3.536
1543+489......	*4.8	3.2	64.9	75.1	1.33	42.11	41.76	−0.35	−5.808
1552+085......	3.5	<0.4	57.3	57.1	1.10	41.49	<40.72	−0.77	−5.581
1612+261......	*103.9	15.5	*83.8	23.7	*0.29	43.05	42.31	−0.74	5.989
2304+042......	*52.0	6.7	117.7	*38.8	*0.32	41.71	40.59	−1.12	2.021

[a] [O III] and [O II] line luminosities are in log (ergs s^{-1}) and were calculated assuming $H_0 = 50$ km s^{-1} Mpc^{-1}, $q_0 = 0$. L([O III]), L([O II]), and [O II]/[O III] ratios are listed in logarithmic units.

[b] The equivalent widths are in Å and the errors are $\sim 15\%-20\%$. The measurements of line equivalent widths and Fe II/Hβ ratio agree with BG92 values to within 30% except where noted by an asterisk.

[c] BG92.

(which in turn reference a star through a 5″ aperture). The amount of starlight for many PG quasars has been measured by McLeod & Rieke (1994a, 1994b). We found that for most of the objects in our sample the starlight contribution is of the order of 20% of the total flux in the H (1.65 μm) band, i.e., 13% at 4000 Å, assuming a starlight template from Elvis et al. (1994). However, PG 0157+001 has a 43% starlight contribution at H band (i.e., 29% at 4000 Å) and is

also spatially extended ($12'' \times 12''$). Assuming a uniform distribution of starlight and a constant AGN energy output, we can roughly estimate the starlight contribution in this (worst-case scenario) object, which is 7% ($0.43 \times 5^2/12^2$) at H band and 5% ($0.29 \times 5^2/12^2$) at 4000 Å in our spectra, and 0.7% and 0.5%, respectively, in BG92 spectra. Hence, the level of starlight contamination in ours and the BG92 equivalent widths is well below the typical 30% errors as a
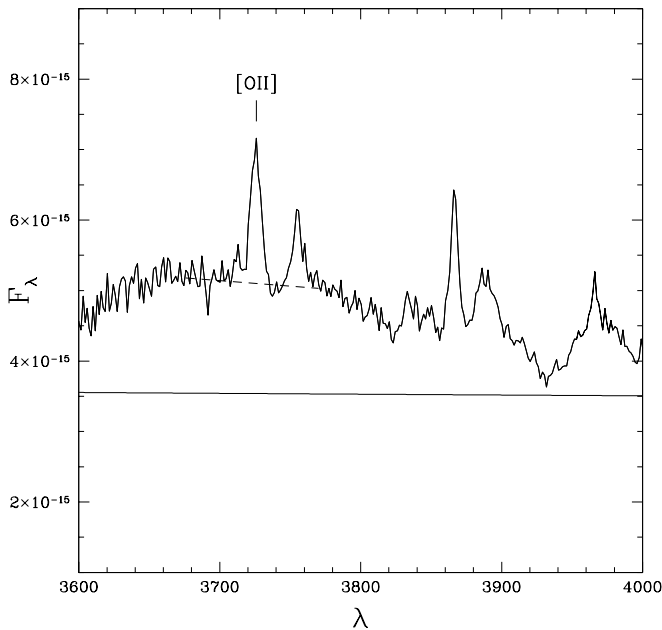

FIG. 3.—Spectrum of PG 0923+129 around the [O II] line. The local continuum representing the continuum from the "small bump" is indicated by a dashed line, while the power-law continuum fitted to the whole spectrum and lying well below the "small bump" is shown by a solid line.
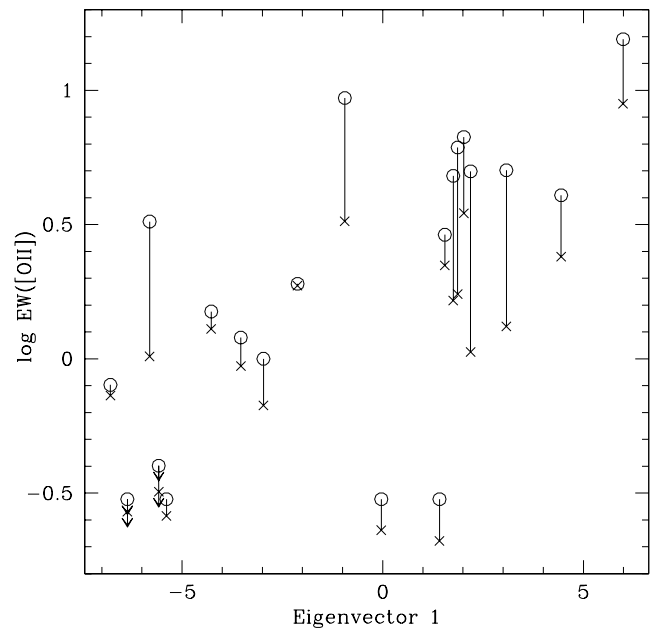

FIG. 4.—[O II] equivalent width vs. the BG92 EV1. Circles denote our equivalent width measurements with respect to our fitted underlying continuum, and crosses denote equivalent width measurements relative to the local continuum, i.e., with the small bump not taken into account.

result of other factors such as continuum placement and line measurement.

2.3. *Eigenvector 1*

The EV1 values for our sample QSOs (kindly provided by T. Boroson) were calculated by applying the PCA analysis to the BQS QSO sample. We quote these values (after BG92) in the last column of Table 2. EV1 was shown by BG92 to depend strongly on the peak and absolute magnitude of the [O III] line ($M_{[O\,III]}$) and the Fe II/Hβ ratio. In general, our line measurements agree well (to within 30%) with those of BG92, implying that it is valid to use the EV1 values from BG92. In Figure 5 we present a comparison of the [O III] luminosity measured by us and the absolute magnitude $M_{[O\,III]}$ from BG92, defined as $M_V - 2.5 \log$ EW([O III]). The general agreement is good, with only one highly discrepant object: PG 1543+489 (indicated in Fig. 5 by a filled circle; see § 2.2 for further explanation of the differences between ours and the BG92 measurements). In four other objects (PG 0157+001, PG 0953+414, PG 1612+261, and PG 2304+042) we measured the Fe II/Hβ ratio to be significantly larger ($>$30%) than in BG92 (see Table 2 and Fig. 6). A comparison of our line equivalent width measurements in these objects indicates that we have set the underlying continuum lower and with a flatter slope in our objects, probably as a result of the fact that our spectra cover a larger wavelength range and that we iterated over the continuum setting and Fe II models in the Fe II subtraction process. In PG 0052+251 the Fe II/Hβ measured by us is smaller than in BG92. However, in our Fe II–subtracted spectrum we still have some residual Fe II λ4570 emission left (as our primary goal was to optimize the Fe II fit around the [O III] line and not Fe II λ4570), so the BG92 Fe II measurement and hence EV1 are probably more correct.

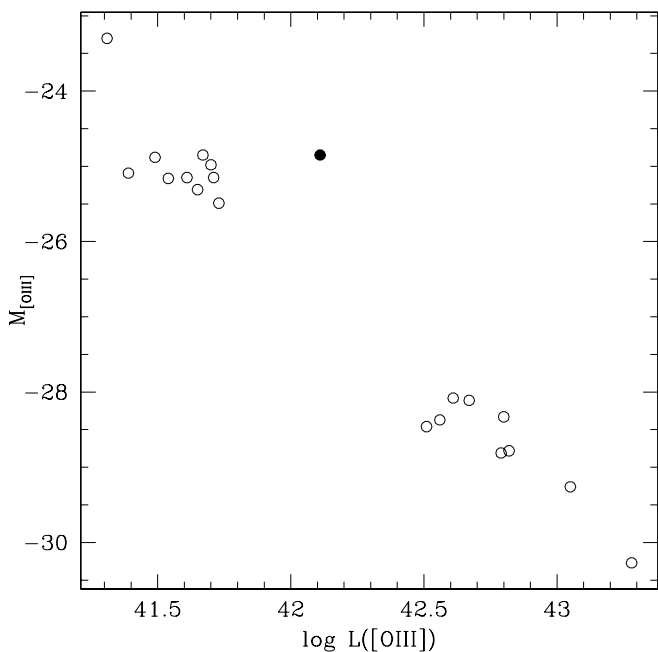FIG. 5.—[O III] absolute magnitude ($M_{[O\,III]}$) from BG92 vs. our [O III] luminosity measurements demonstrating good agreement. The filled circle represents PG 1543+489, for which the BG92 measurement of EW([O III]) is inconsistent with ours.
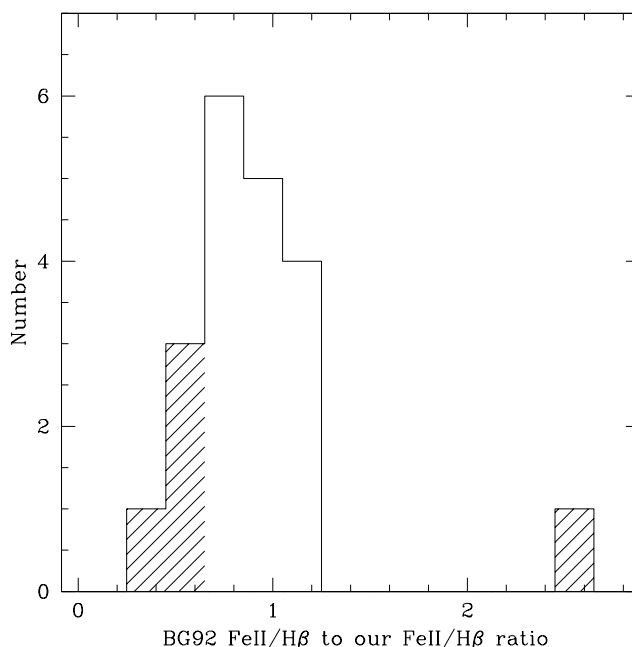

FIG. 6.—Histogram of the ratio Fe II/Hβ measured by BG92 to the Fe II/Hβ ratio measured by us. Shaded areas denote quasars for which our Fe II/Hβ measurements differed from BG92 by at least 30%.

For the five discrepant objects discussed above, we indicate the direction in which EV1 should move in our figures based on the EV1 range of objects with similar values of Fe II/Hβ, $M_{[O\,III]}$, and [O III] peak measurements in BG92. The only way to improve on this would be to rerun the PCA analysis for the full BG92 sample using our new values of line measurements, which is beyond the scope of this paper.

3. DISCUSSION

As outlined in the Introduction, the differences in [O III] emission between the narrow-line radio galaxies and radio-loud quasars reported by Jackson & Browne (1990) and lack thereof in [O II] (Hes et al. 1996) suggest that [O III] is orientation dependent while [O II] is more isotropic in the radio-loud AGN. The correlation between the [O II]/[O III] ratio and the orientation indicator R reported by B97 furthermore suggests orientation-dependent dust obscuration of [O III] emission and more isotropic [O II] emission. These results question the BG92 conclusion that EV1 is independent of orientation based on the assumption of [O III] isotropy and allow us to readdress the question of orientation as the driver of EV1 by studying the dependence of BG92 EV1 on isotropic [O II] emission. To ensure a wide range in EV1 values, we selected radio-quiet quasars with either high or low [O III] luminosities (see § 2). Under the assumption that our radio-quiet quasars, which are a subset of the BQS sample, have similar narrow-line–emitting regions to the radio-loud quasars and powerful radio-loud galaxies, we presume that [O II] emission is independent of orientation in radio-quiet quasars. As a result, finding a strong relation between EV1 and [O II] luminosity would imply that EV1 is independent of orientation (furthermore suggesting isotropic [O III] emission in radio-quiet quasars, as [O III] correlates with EV1), while the lack of such a relation would suggest that orientation is a factor.

The relations between [O III] and [O II] luminosities [L([O III]), L([O II])] and the BG92 EV1 are presented

in Figure 7. We find a significant correlation between $L([\text{O III}])$ and EV1 consistent with the $M_{[\text{O III}]}$ versus EV1 correlation found by BG92. The Spearman rank test shows a 0.09% probability of this correlation occurring by chance (hereafter we will use P_S to indicate the chance probability in the Spearman rank test[4]). We also find a significant correlation between $L([\text{O II}])$ and EV1 with $P_S = 0.23\%$, which becomes stronger with $P_S = 0.08\%$ if the values of EV1 were updated to allow for the differences between our measurements and those of BG92 (i.e., values in the range shown by the arrows in Fig. 7). These results imply that EV1 is independent of orientation and suggest that an intrinsic property, such as the accretion rate onto a black hole (as suggested by BG92; Pounds, Done, & Osborne 1995; Boller, Brandt, & Fink 1996; Laor et al. 1997) or the black hole spin (BG92), may be driving EV1. In Figure 8 we present the spectra around the [O II] wavelength for the most positive and the most negative EV1 objects to show in detail the dependence of [O II] on EV1.

3.1. Radio-quiet versus Radio-loud Quasars

The presence of the correlations between $L([\text{O II}])$, $L([\text{O III}])$, and EV1 found above suggest that in our radio-quiet quasars from the BQS sample the [O III] emission is independent of orientation in contrast to the case of radio-loud quasars. In order to understand this apparent dichotomy, we study in detail the $L([\text{O II}])$ versus $L[\text{O III}]$ and EW([O III]) versus EW([O II]) relations in our radio-quiet sample and compare it with the radio-loud samples of B97

---

[4] We use the ASURV statistical package (Isobe, Feigelson, & Nelson 1986), which includes allowance for the presence of upper limits in [O II] measurements.
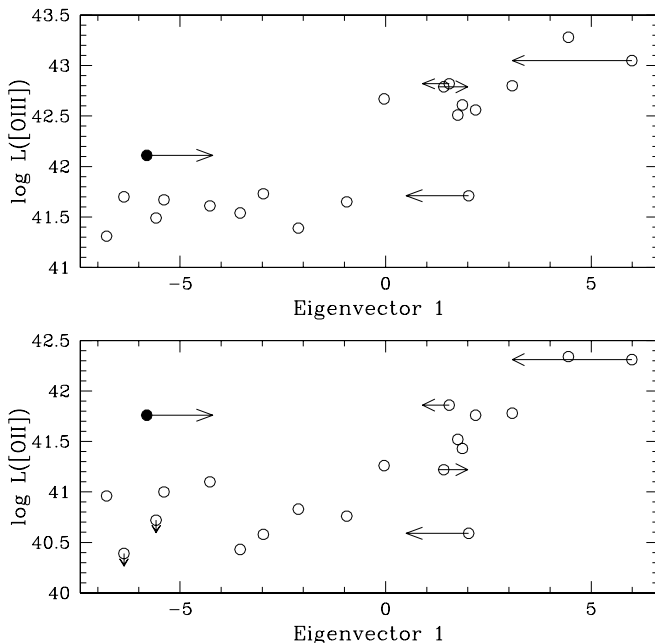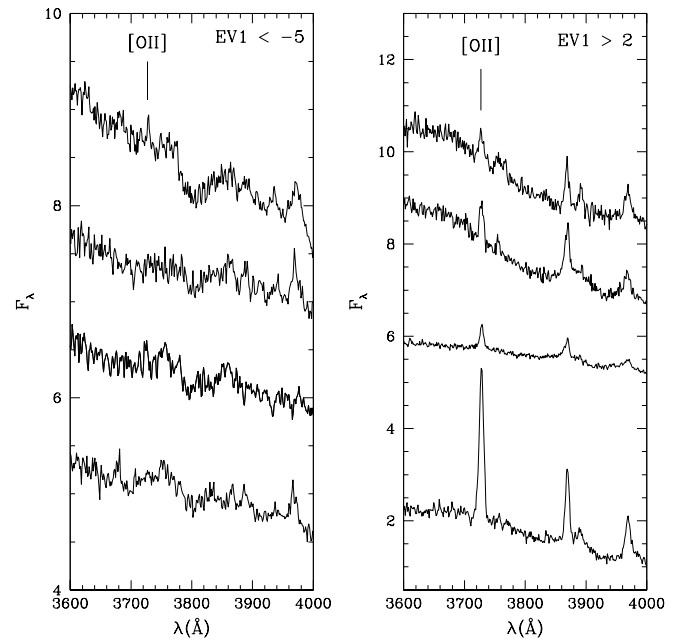

FIG. 8.—Observed spectra in the rest frame showing in detail the wavelength range around the [O II] line for the most extreme EV1 objects on a scale F_λ (in units of 10^{-15} ergs s^{-1} cm^{-2} Å^{-1}) as a function of λ (Å). Spectra have been shifted downward by an arbitrary value for clarity. The left panel shows objects with EV1 < −5 (*top to bottom*: PG 1402+261, PG 1404+226, PG 1415+451, PG 1552+085), and the right panel shows objects with EV1 > 2 (*top to bottom*: PG 0026+129, PG 0052+251, PG 1049−005, PG 1612+261).

FIG. 7.—[O III] and [O II] luminosity vs. BG92 EV1 correlations. PG 1543+489 is shown as a filled circle. Arrows indicate a range of EV1 values for PG 0157+001, PG 0953+414, PG 1543+489, PG 1612+261, and PG 2304+042 based upon our differing line measurements in comparison with BG92.

and Tadhunter et al. (1998), where orientation combined with dust or ionization effects, respectively, were found to be present.

The [O II] and [O III] luminosities and equivalent widths in our radio-quiet sample correlate significantly with one another [$P_S = 0.04\%$ for $L([\text{O III}])$ vs. $L([\text{O II}])$ correlation and $P_S = 0.31\%$ for EW([O III]) vs. EW([O II]) correlation]. Additionally, the range in $L([\text{O II}])$ and $L([\text{O III}])$ is similar (~ 2 dex), and the best-fitted linear regression slope is consistent with 1 within the errors [0.84 ± 0.11 for $L([\text{O II}])$ vs. $L([\text{O III}])$ and 1.27 ± 0.37 for $L([\text{O III}])$ vs. $L([\text{O II}])$; see Fig. 9]. The range in equivalent widths is also similar [1.6 dex for EW([O III]) and 1.7 dex for EW([O II])].

If our sample was affected by orientation-dependent dust obscuration (where, as in B97, substantial numbers of dust clouds lie within the torus opening angle, and their number increases toward the plane of the torus), a larger range in $L([\text{O III}])$ than in $L([\text{O II}])$ would be observed, as a result of the obscuration of [O III] emission at large inclination angles. Additionally, a smaller range in EW([O III]) than in EW([O II]) would be expected as a result of the orientation-dependent dust reddening of the continuum and the [O III] emission. If, on the other hand, only ionization effects were present in our sample, we would observe a larger range in $L([\text{O III}])$ than in $L([\text{O II}])$ and a larger range in EW([O III]) than in EW([O II]), as the [O III] line is much more dependent on the ionization parameter U than [O II] (see, e.g., Simpson 1998, Fig. 5). Neither effect is present in our sample, suggesting that the BQS quasars (at least our radio-quiet sample) are remarkably free of orientation-dependent dust effects or ionization effects in the narrow-line region.
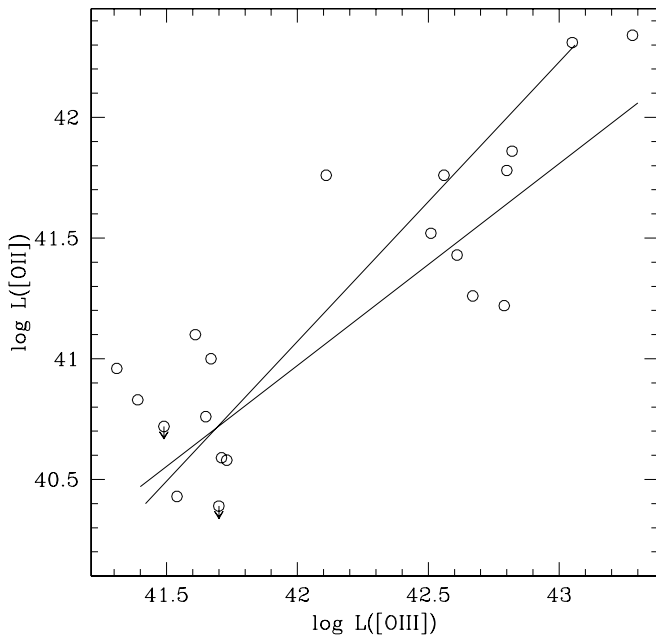
FIG. 9.—[O II] luminosity vs. [O III] luminosity correlation

selected quasar sample (Figs. 10a and 11a) and the complete sample of southern 2 Jy radio sources presented by Tadhunter et al. (1998; Figs. 10b and 11b). A number of B97 quasars and almost all broad- and narrow-line radio galaxies of Tadhunter et al. (1998) are found to occupy a region of higher EW([O II]) and EW([O III]) (see Figs. 10a and 10b) than our radio-quiet quasars. We found that these comparison objects cover the whole range of [O III] and [O II] luminosities, indicating that the high equivalent widths of the radio-loud objects are due either to higher [O III] and [O II] luminosities or to lower observed continuum. In the latter case the continuum could be obscured by dust in the radio-selected AGN. This would confirm previous suggestions (based on the comparison of the BQS quasars' optical slopes [Francis et al. 1991] with the X-ray–selected RIXOS sample of Puchnarewicz et al. 1996 and a heterogeneous sample of Elvis et al. 1994) that the blue color selection of the BQS QSOs biases against dust-obscured objects, while radio selection is unaffected.

Figures 10a and 11a also show that our sample extends to lower EW([O III]) and L([O III]) than B97 while having similar minimum values of EW([O II]) and L([O II]). The [O II] was measured with respect to the underlying continuum in both samples, and the lowest values are at the detection limit. It is possible that the [O III] emission may be overestimated in the lowest equivalent width/luminosity B97 objects as a result of the lack of Fe II subtraction. For the extremely strong Fe II objects in our radio-quiet sample, the equivalent width and luminosity of [O III] would be overestimated by a factor of up to 10 if the Fe II emission were not subtracted [e.g., for PG 1402+261 EW([O III]) = 36 with Fe II included and EW([O III]) = 3 after Fe II subtraction]. Correction for Fe II contamination

As both the [O II] and [O III] emission are independent of orientation effects, the [O II]/[O III] ratio in these optically selected radio-quiet quasars is not an orientation indicator, contrary to results for radio-loud AGNs.

We compare the equivalent widths and luminosities of [O III] and [O II] lines of objects in our optically selected radio-quiet sample with the B97 low-frequency radio-
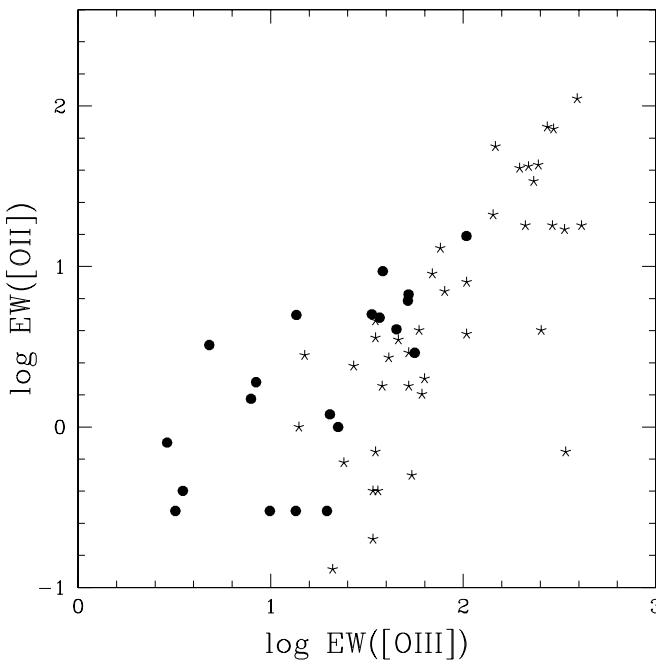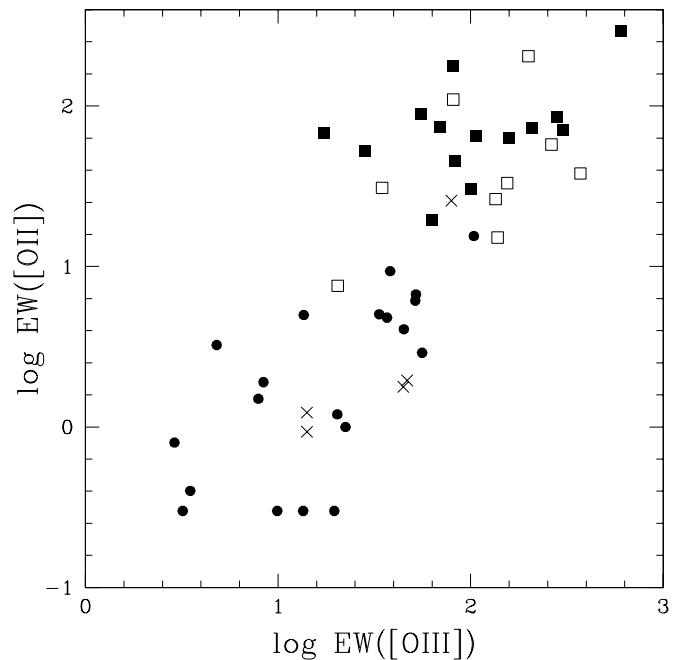

FIG. 10a

FIG. 10b

FIG. 10.—(a) Comparison of the [O III] and [O II] equivalent widths of our sample (filled circles) with those of B97 (asterisks). Our sample extends to smaller EW([O III]) than B97, probably because of our Fe II subtraction. The EW([O III]) can be overestimated by up to a factor of 10 in strong Fe II/weak [O III] sources (see text) if Fe II is not subtracted. (b) Comparison of the [O III] and [O II] equivalent widths of our sample (filled circles) with those of Tadhunter et al. (1998) (crosses: quasars; open squares: broad-line radio galaxies; filled squares: narrow-line radio galaxies).
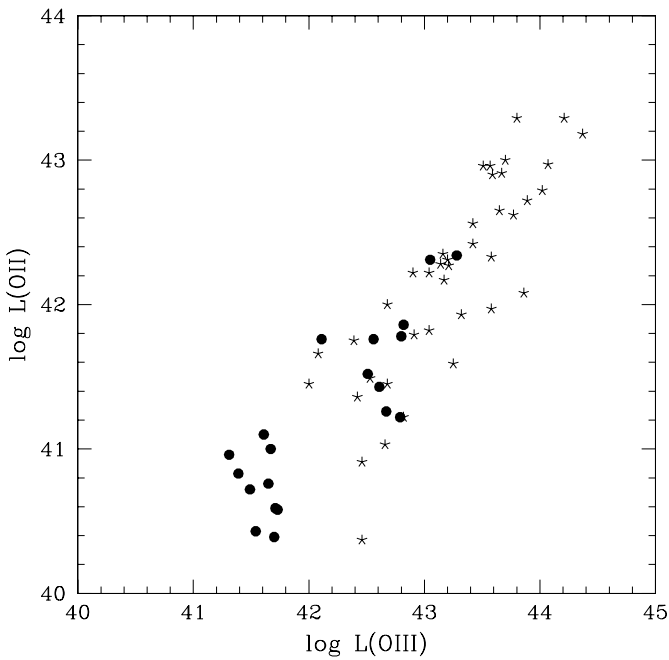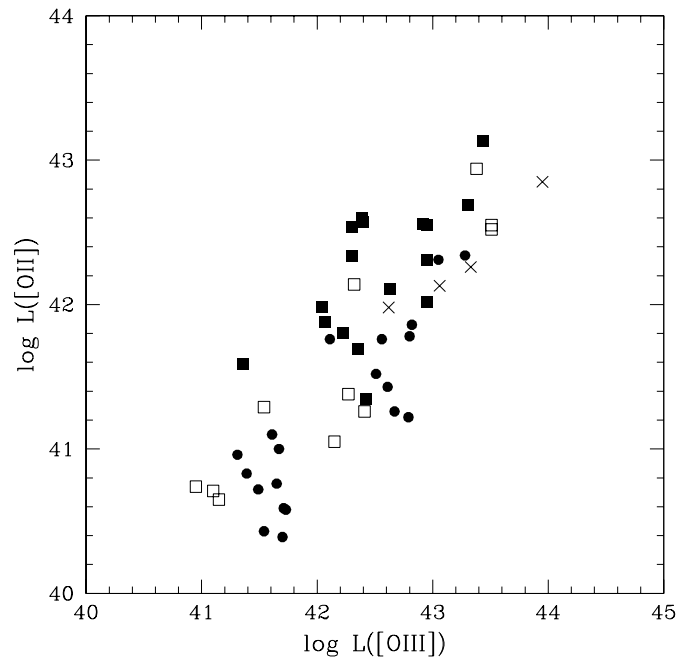
FIG. 11a

FIG. 11b

FIG. 11.—(a) Comparison of the [O III] and [O II] luminosities of our sample (*filled circles*) with those of B97 (*asterisks*). (b) Comparison of [O III] and [O II] luminosities of our sample (*filled circles*) with those of Tadhunter et al. (1998) (*crosses*: quasars; *open squares*: broad-line radio galaxies; *filled squares*: narrow-line radio galaxies).

in the B97 sample could potentially result in an intrinsic range of EW([O III]) and L([O III]) larger (by a factor of 10) than shown in Figures 10a and 11a and comparable to the range of EW([O II]) and L([O II]), respectively. This would

suggest (contrary to the conclusion reached by the author) that in the B97 sample there is no dust obscuring the inner region of [O III] emission. Confirmation of this suggestion would require a reanalysis of the B97 sample. However, to
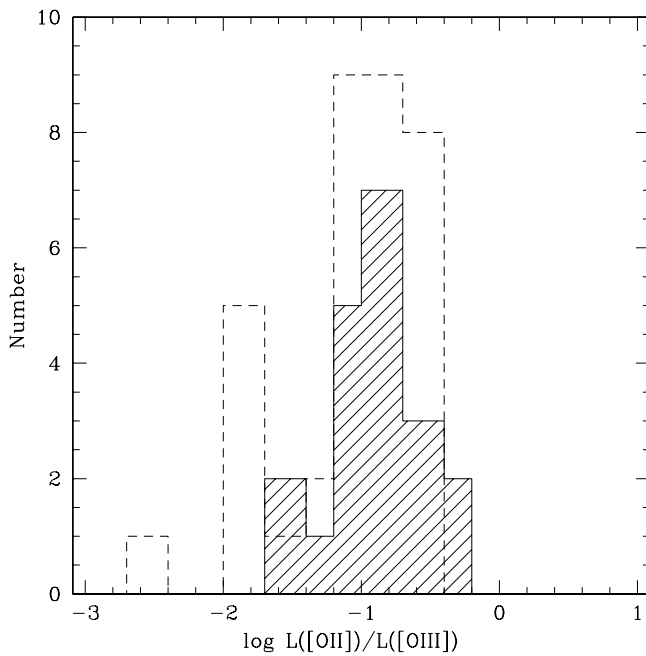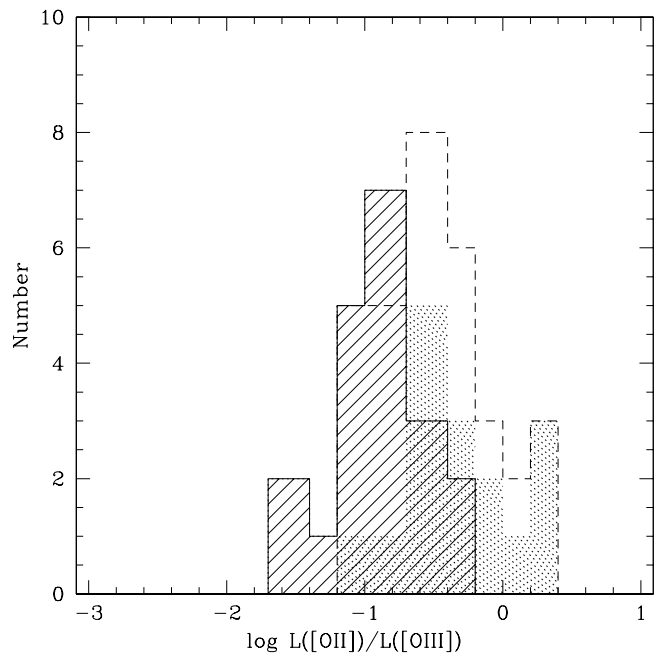

FIG. 12a

FIG. 12b

FIG. 12.—(a) Histogram of the [O II]/[O III] luminosity ratio. Area shaded with solid lines indicates L[O II]/L[O III] ratios for our sample, and unshaded, dashed contours are radio-loud quasars from B97. (b) Histogram of the [O II]/[O III] luminosity ratio. Area shaded with solid lines indicates L[O II]/L[O III] ratios for our sample, and dashed contours are powerful radio galaxies from Tadhunter et al. (1998). The area shaded with dotted lines indicates the narrow-line radio galaxies within the Tadhunter et al. (1998) sample.

account for the broad-line and continuum reddening observed by B97, dust between the broad-line and the narrow-line region is still needed.

3.2. *The* [O II]/[O III] *Ratio as an Orientation Indicator*

In the previous section we concluded that the [O II]/[O III] ratio is not an orientation indicator in our radio-quiet BQS sample. In this section we address the issue of the [O II]/[O III] ratio as an orientation measure in radio-loud quasars.

The comparison of [O II]/[O III] ratios with B97 (Fig. 12a) shows a lack of objects in our sample with the lowest values of [O II]/[O III] ratio, i.e., surprisingly the most core-dominated objects in B97. One possibility is an overestimation of the [O III] emission in B97 data resulting from Fe II contamination, as discussed above, which may be the case for four quasars with the smallest EW([O III]) (see also Baker et al. 1999 for spectra). Core-dominated radio-loud quasars have stronger Fe II emission than lobe-dominated quasars (e.g., Miley & Miller 1979), so the Fe II contamination would be larger in core-dominated objects, leading to higher apparent [O III] luminosity (as observed by Jackson & Browne 1990) and lower [O II]/[O III] ratios in B97. In this case, the [O II]/[O III] versus R relation of B97 could be caused by the orientation dependence of Fe II rather than of [O III].

Another possible cause of low [O II]/[O III] ratios in the B97 sample [which could be the case for two quasars with extremely large EW([O III])] is a higher ionization parameter in radio-loud quasars. A comparison of our subset of the BQS sample and the B97 low-frequency radio-selected quasar sample, with the complete sample of 2 Jy radio sources presented by Tadhunter et al. (1998), shows that both ours and the B97 sample lack objects with the highest [O II]/[O III] ratios (log $[L([O II])/L([O III])] > 0$; see Fig. 12b). These high [O II]/[O III] objects in Tadhunter et al. (1998) are mostly narrow-line radio galaxies (see Fig. 12b) believed to be edge-on AGNs. These objects are expected to have a large fraction of the [O III] nuclear emission obscured by the dusty torus, resulting in a higher [O II]/[O III] ratio. However, there are also narrow-line radio galaxies (in Fig. 12b) that show values of $L([O II])/L([O III]) < 0$, within the range of ours and the B97 quasars, as well as the broad-line radio galaxies from Tadhunter et al. (1998). This seems to be inconsistent with the orientation-dependent [O III] scenario in powerful radio-loud galaxies and suggests that the [O II]/[O III] ratio instead depends on the ionization parameter U, as suggested by Tadhunter et al. (1998).

Based on our comparisons, we conclude that the [O II]/[O III] ratio is not a reliable orientation indicator either in the radio-quiet sample of the BQS quasars or in the radio-loud quasars.

4. CONCLUSIONS

Until recently it was generally accepted that EV1 does not depend on orientation, as it is strongly correlated with [O III] emission, originally thought to be an isotropic property in quasars. As recent studies of radio-selected AGN samples have questioned the isotropy of [O III] emission, we have investigated the relation between [O II] emission, which appears to be more isotropic, and EV1, and once again addressed the question of orientation as a driver of EV1.

We chose radio-quiet quasars from the optically selected BQS that showed either high or low [O III] luminosity, spanning a wide range of EV1 values in BG92. We subtracted Fe II emission, which contaminates the [O III] emission, from our spectra (using the BG92 iron template). We also demonstrated the significant effect of the presence of the small blue bump (Balmer continuum and Fe II emission) on accurate measurements of the [O II] emission line, emphasizing the need for spectra covering a wide (≥ 1000 Å) wavelength range in order to determine the underlying continuum.

We found the following:

1. Strong correlations between $L([O II])$, $L([O III])$, and EV1, implying that EV1 does not depend on orientation, confirming earlier conclusions of BG92 and Boroson (1992), based on [O III] alone. EV1 is likely driven by an intrinsic property (e.g., accretion rate or black hole spin).
2. Significant EW([O III])-EW([O II]) and $L([O III])$-$L([O II])$ correlations.
3. Similar ranges in EW([O III]) and EW([O II]) and in $L([O III])$ and $L([O II])$, respectively.

These results lead us to conclude that the optically selected BQS sample (at least our radio-quiet sample) is free from orientation-dependent dust effects and ionization-dependent effects in the narrow-line region. Assuming that our sample is representative of bright, optically selected radio-quiet quasars, this implies that their [O III] emission is isotropic and that the [O II]/[O III] ratio is not an orientation indicator. This is in contrast with earlier results for the radio-selected AGN (B97; Jackson & Browne 1990). We suggest that this discrepancy may be due to contamination of the [O III] emission by orientation-dependent Fe II emission in the latter samples.

REFERENCES

Antonucci, R. 1993, ARA&A, 31, 473
Baker, J. C. 1997, MNRAS, 286, 23 (B97)
Baker, J. C., Hunstead, R. W., Kapahi, V. K., & Subrahmanya, C. R. 1999, ApJS, 122, 29
Barth, A. J., Tran, H. D., Brotherton, M. S., Filippenko, A. V., Ho, L. C., van Breugel, W., Antonucci, R., & Goodrich, R. W. 1999, AJ, 118, 1609
Boller, T., Brandt, W. N., & Fink, H. 1996, A&A, 305, 53
Boroson, T. A. 1992, ApJ, 399, 15
Boroson, T. A., & Green, R. F. 1992, ApJS, 80, 109 (BG92)
Brandt, N., & Boller, Th. 1998, Astron. Nach., 319, 163
Corbin, M. R. 1993, ApJ, 403, L9
di Serego Alighieri, S., Cimatti, A., Fosbury, R. A. E., & Hes, R. 1997, A&A, 328, 510
Elvis, M., et al. 1994, ApJS, 95, 1

Francis, P. J., Hewett, P. C., Foltz, C. B., Chaffee, F. H., Weymann, R. J., & Morris, S. L. 1991, ApJ, 373, 465

Giveon, U., Maoz, D., Kaspi, Sh., Netzer, H., & Smith, P. S. 1999, MNRAS, 306, 637

Hes, R., Barthel, P. D., & Fosbury, R. E. A. 1996, A&A, 313, 423

Isobe, T., Feigelson, E. D., & Nelson, P. I. 1986, ApJ, 306, 490

Jackson, N., & Browne, I. W. A. 1990, Nature, 343, 43

Keel, W. C., Grijp, M. H. K., Miley, G. K., & Zheng, W. 1994, A&A, 283, 791

Kuraszkiewicz, J., Wilkes, B. J., Czerny, B., & Mathur, S. 2000, ApJ, in press

Laor, A., Fiore, F., Elvis, M., Wilkes, B. J., & McDowell, J. C. 1994, ApJ, 435, 611

———. 1997, ApJ, 477, 93

Lawrence, A. 1987, PASP, 99, 309

McLeod, K. K., & Rieke, G. H. 1994a, ApJ, 431, 137

———. 1994b, ApJ, 420, 58

Miley, G. K., & Miller, J. S. 1979, ApJ, 228, L55

Pounds, K. A., Done, C., & Osborne, J. P. 1995, MNRAS, 277, L5

Puchnarewicz, E. M., et al. 1996, MNRAS, 281, 1243

Schmidt, M., & Green, R. F. 1983, ApJ, 269, 352

Simpson, C. 1998, MNRAS, 297, L39

Tadhunter, C. N., Morganti, R., Robinson, A., Dickson, R., Villar-Martin, M., & Fosbury, R. A. 1998, MNRAS, 298, 1035

Tokarz, S. P., & Roll, J. 1997, in ASP Conf. Ser. 125, Astronomical Data Analysis Software and Systems, ed. G. Hunt & H. E. Payne (San Francisco: ASP), 140

Vestergaard, M., & Wilkes, B. J. 2000, ApJ, submitted

Vestergaard, M., Wilkes, B. J., & Barthel, P. D. 2000, ApJL, submitted

Wall, J., & Peacock, J. 1985a, ApJ, 302, 56

———. 1985b, MNRAS, 216, 173

Wilkes, B. J., Schmidt, G. D., Smith, P. S., Mathur, S., & McLeod, K. K. 1995, ApJ, 455, L13

Wills, B. J., Brotherton, M. S. M., Laor, A., Wills, D., Wilkes, B. J., Ferland, G. J., & Shang, Z. 1999, in ASP Conf. Ser. 162, Quasars and Cosmology, ed. G. Ferland & J. Baldwin (San Francisco: ASP), 373

Wills, B. J., & Browne, I. W. A. 1986, ApJ, 302, 56